Parametric Modeling and Structural Optimization of Mechanical Components: Ensuring Assembly Compatibility and Minimizing Failure Risks

Can Ulas Dogruer[1] and Bora Yıldırım [2]

***Abstract*— This study presents an integrated approach to the parametric modeling and structural optimization of mechanical components, emphasizing assembly compatibility and failure risk minimization. The parametric modeling is conducted in CAD software, leveraging its robust CAD capabilities to create flexible, parameter-driven component designs. Finite element analysis (FEA) and multi-objective optimization are performed in MATLAB, utilizing its computational power to evaluate and enhance the mechanical performance of the components. A seamless communication framework between CAD software and MATLAB is established to enable an iterative optimization cycle. The optimization process aims to minimize natural frequency deviations, stress, strain and deformation, while ensuring that the components adhere to strict assembly constraints and maintain structural integrity. This methodology demonstrates an efficient workflow for designing mechanically optimized components that meet both functional and assembly requirements. Unlike previous studies that address structural performance and assembly constraints separately, this work explicitly integrates both within a unified optimization loop, providing a practical and scalable solution for real-world shaft design problems. The proposed framework is validated through case studies, showcasing its effectiveness in improving performance and reducing failure risks in mechanical systems.**

I. Introduction

The design and optimization of mechanical components are critical to achieving efficient, reliable, and manufacturable engineering systems. In particular, shafts play a pivotal role in mechanical systems, transmitting torque, resisting deformation, and interacting with neighboring components. Designing such components requires balancing multiple conflicting objectives, including minimizing stress, deformation, reaction forces, and volume, while adhering to assembly constraints and ensuring structural integrity. Achieving this balance necessitates a robust and integrated framework that combines parametric modeling, finite element analysis (FEA), and optimization.

Modern parametric modeling tools like CAD software facilitate the creation of flexible, parameter-driven designs that can be iteratively optimized. Coupled with MATLAB's computational capabilities for FEA and optimization, these tools provide a powerful platform for addressing multi-objective mechanical design problems. This study focuses on integrating these platforms into a unified framework for shaft design optimization. The framework iteratively minimizes critical metrics such as stress and deformation while ensuring that dimensional and functional constraints for assembly are satisfied.

The foundations for this research are rooted in several key studies. Early contributions by Bendsoe [1] and Sigmund [2] laid the groundwork for topology optimization, which has since evolved into more comprehensive frameworks combining topology, size, and shape optimization [3], [4]. Kulkarni et al. [5] and Gupta et al. [6] explored the application of meta-heuristic algorithms, such as particle swarm optimization (PSO), highlighting their effectiveness in solving complex engineering problems. Studies by Saitou et al. [7], Arora [8], and Lu and Chen [9] emphasized the importance of incorporating manufacturability and assembly constraints into optimization frameworks. Recent advances have also included approaches to additive manufacturing [10], [11], and innovative applications of FEA for specific components like shafts and connecting rods [12], [13].

Although various studies have utilized CAD or FEA independently in shaft design, few have combined them within a feedback-based iterative optimization loop that accounts for both structural performance and assembly fit. This study fills this methodological gap by systematically integrating parametric CAD geometry, automated FEA evaluation, and multi-objective optimization under real-world constraints

This article presents a structured study on the optimization of shaft design in mechanical systems, combining theoretical insight with practical implementation. In Section I, the significance of addressing stress concentrations, deformation, and resonance is outlined, emphasizing the role of FEA and computational optimization. Section II surveys related work in structural and meta heuristic optimization, identifying the need for an integrated design framework. Section III defines the multi-objective problem with a focus on mechanical efficiency and assembly constraints. Theoretical foundations such as stress analysis, deformation limits, and modal behavior are presented in Section IV. An integrated computational approach linking parametric CAD modeling, FEA, and genetic algorithms is introduced in Section IV. The case study in Section V demonstrates clear improvements in

*This study was supported by the *Hacettepe University Scientific Research Projects Coordination Unit* under the project code FHD-2024-21284. The project, titled *Matlab and CAD Programs in the Topology Optimization Cycle: Structural Parametric Optimization of Mechanical Parts*, provided the infrastructure and resources essential for this research. The authors sincerely thank the Coordination Unit for their support and contributions.

[1]Can Ulas Dogruer is with Department of Mechanical Engineering, Hacettepe University, 06800, Ankara, Turkey. cdogruer@hacettepe.ed.tr; ORCID: 0000-0001-8916-931X

[2] Bora Yıldırım is with Department of Mechanical Engineering, Hacettepe University, 06800, Ankara, Turkey. boray@hacettepe.ed.tr; ORCID: 0000-0003-3293-9656

stress distribution, deflection control, and modal separation. Concluding in Section VI, the study confirms that combining modern simulation tools with meta heuristic optimization enhances both reliability and manufacturability in shaft design.

II. Related Works

Structural optimization has witnessed substantial progress over the decades, with methods evolving from traditional approaches to advanced multi-objective frameworks. The pioneering work by Bendsoe [1] on topology optimization introduced a material distribution approach, further refined by Sigmund [2] to address structural tailoring for performance improvement. Zhou et al. [3] and Christiansen et al. [4] extended these ideas by integrating topology, size, and shape optimization, enabling more comprehensive designs for mechanical components.

Meta-heuristic algorithms have emerged as powerful tools for addressing complex optimization problems. Kulkarni et al. [5] reviewed the application of PSO in mechanical engineering, while Gupta et al. [6] conducted a comparative analysis of various optimization techniques. Rao et al. [14] introduced the Teaching–Learning-Based Optimization method, which demonstrated strong performance in constrained optimization problems. Sun et al. [15] extended these methods to robust optimization under uncertain conditions, showcasing their adaptability to real-world applications.

Specific to mechanical components, several studies have applied optimization techniques to shafts and related structures. Shinde and Sawant [16] focused on drive shafts, optimizing them for torsional strength and fuel efficiency, while Shanmugasundar et al. [12] explored topology optimization for connecting rods. Noordman et al. [11] demonstrated the application of topology optimization to 3D-printed shafts, emphasizing the potential of additive manufacturing. Similarly, Pinelli et al. [10] examined lightweight designs for turbine blades, leveraging topology optimization in additive manufacturing workflows.

Assembly constraints, a critical aspect of mechanical design, have been explored by Cheng and Maghsoodloo [17], who optimized tolerances using Taguchi's quality loss function. Tang and Chang [18] addressed the integration of topology and shape optimization highlighting its importance in ensuring proper functionality. Recent works have incorporated innovative techniques, such as optimization [19], to enhance the structural and functional performance of mechanical components.

This study builds on these advancements by providing a unified framework that integrates parametric modeling, FEA, and optimization for shaft design. Unlike prior works, which often treat structural performance and assembly constraints independently, this article explicitly addresses their interplay, demonstrating the practical applicability of the proposed framework through a detailed case study.

Prior works have generally optimized structural or assembly parameters in isolation. In contrast, the present study unifies parameterized geometry, modal constraints, and mechanical performance goals under a single cost function within a tightly coupled simulation optimization loop. This comprehensive integration is rarely seen in literature, particularly for rotating components such as shafts

III. Problem Statement

Despite significant advancements in the optimization of mechanical components, several challenges remain. Existing studies often treat structural performance and assembly constraints as separate entities, leading to sub-optimal designs when these factors interact. Additionally, the practical integration of parametric modeling tools like CAD software with optimization and FEA platforms such as MATLAB is under-explored, particularly in the context of iterative design cycles.

Shaft design presents unique challenges, requiring a careful balance between structural objectives (e.g., minimizing stress, deformation, and volume) and functional requirements (e.g., assembly constraints and failure minimization). Traditional optimization methods often overlook these interactions, resulting in designs that fail to meet practical requirements in complex systems.

This study addresses these challenges by developing a robust framework that integrates parametric modeling, FEA, and multi-objective optimization. By explicitly incorporating assembly constraints into the optimization process, the proposed framework ensures compatibility with neighboring components while achieving high structural performance. The framework is demonstrated through a practical case study on shaft design, providing a novel approach to solving real-world mechanical design problems.

IV. Theory

A. Optimization Theory and Framework

Optimization is a mathematical process of finding the best solution for a given problem under a defined set of constraints. In the context of this study, the optimization problem is structured as a constrained multi-variable optimization problem, where some dimensions of the parametric CAD model, developed in CAD software, serve as the free parameters of optimization.

The objective of the optimization is to minimize a cost function, $J(\mathbf{x})$, which encapsulates key performance criteria such as stress, deformation, volume, and natural frequency. The optimization problem can be expressed as:

$$\min_{\mathbf{x}} J(\mathbf{x}) \quad \text{subject to} \quad \begin{array}{ll} g_i(\mathbf{x}) \leq 0, & i = 1, 2, \ldots, m, \\ h_j(\mathbf{x}) = 0, & j = 1, 2, \ldots, p, \end{array} \tag{1}$$

where:

-$\mathbf{x} = [x_1, x_2, \ldots, x_n]$ represents the free parameters of the CAD model.

- $g_i(\mathbf{x})$ are the inequality constraints limiting the range of free parameters.

- $h_j(\mathbf{x})$ are the equality constraints representing relationships (linear or nonlinear) between free parameters.

The optimization process integrates CAD software for parametric modeling and MATLAB for FEA and optimization. Fig. 1 illustrates the flowchart and general steps of the topology optimization method used in this study. Flowchart illustrates the key software information exchange between the CAD and MATLAB programs. The workflow consists of the following steps:

1. Free Parameter Initialization: Dimensions of the CAD model are selected as free parameters ($\mathbf{x}$), with initial values satisfying all constraints.

2. Setup in MATLAB: The optimization problem is defined in MATLAB, including the cost function $J(\mathbf{x})$, constraints $g_i(\mathbf{x})$ and $h_j(\mathbf{x})$, and boundary conditions.

3. Model Update: At each optimization iteration, free parameters $\mathbf{x}$ are updated in MATLAB. The CAD model in CAD software is modified accordingly and exported as an STL file.

4. Finite Element Analysis: The STL file is imported into MATLAB, where it is meshed, boundary conditions are applied, and loads are defined. FEA is conducted to evaluate structural performance.

5. Cost Function Evaluation: The performance metrics obtained from FEA are used to calculate the cost function $J(\mathbf{x})$.

6. Optimization Cycle: The optimization solver minimizes $J(\mathbf{x})$ iteratively, updating $\mathbf{x}$ while ensuring that all constraints are satisfied.

7. Convergence Check: The process continues until the optimization converges, i.e., the cost function reaches its minimum and all constraints are satisfied.

B. Failure Theorems: Tresca vs. von Mises

Two widely used failure theories for ductile materials are the Maximum Shear Stress Theory (Tresca) and the Distortion Energy Theory (von Mises). Both are employed to predict yielding under complex loading conditions, but they differ in their approach and criteria.

1) Tresca Criterion: The Tresca criterion, also known as the Maximum Shear Stress Theory, states that yielding occurs when the maximum shear stress in a material equals or exceeds the shear stress at yielding in a simple tension test. It is mathematically expressed as:

$$\max\left(|\sigma_1 - \sigma_2|, |\sigma_2 - \sigma_3|, |\sigma_3 - \sigma_1|\right) \geq \sigma_y \tag{2}$$

where:

- $\sigma_1, \sigma_2, \sigma_3$ are the principal stresses ($\sigma_1 \geq \sigma_2 \geq \sigma_3$),
- σ_y is the yield strength of the material.

This criterion assumes that the maximum shear stress governs yielding and provides conservative results [20].

2) von Mises Criterion: The von Mises criterion, or the Distortion Energy Theory, predicts yielding when the distortion energy per unit volume reaches the value at yielding in a simple tension test. It is expressed as:

$$\sigma_{\text{eq}} = \sqrt{\frac{1}{2}\left[(\sigma_1 - \sigma_2)^2 + (\sigma_2 - \sigma_3)^2 + (\sigma_3 - \sigma_1)^2\right]} \tag{3}$$

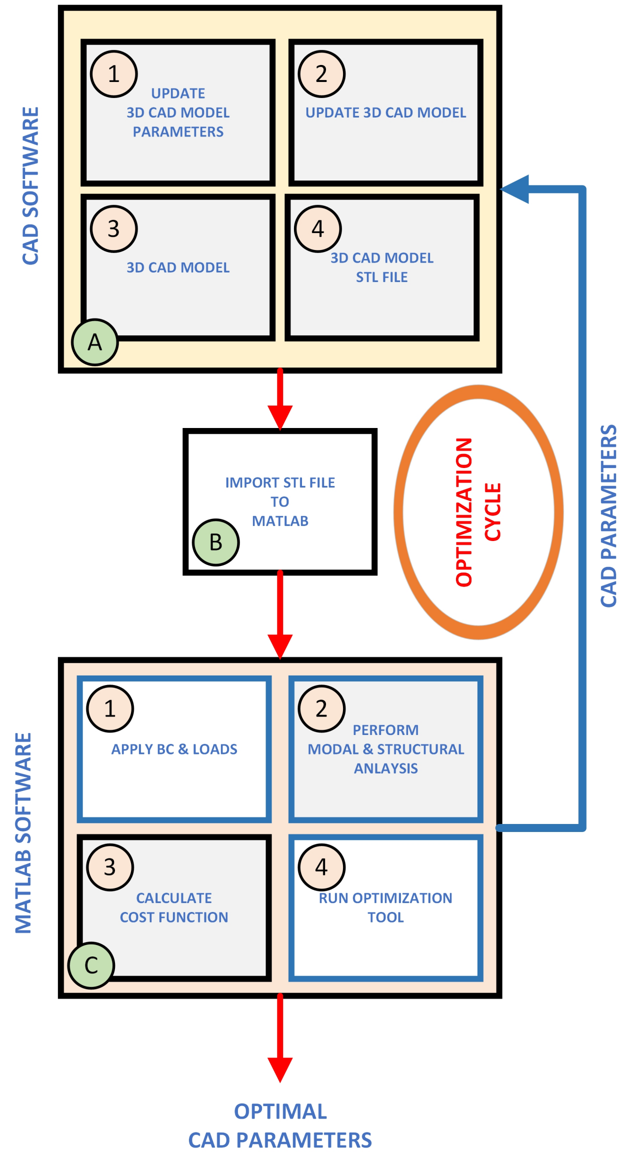

Fig. 1. Flowchart of CAD-MATLAB based structural optimization.

$$\sigma_{\text{eq}} \geq \sigma_y \tag{4}$$

where σ_{eq} is the von Mises equivalent stress.This criterion accounts for the combined effect of all three principal stresses and typically provides less conservative predictions than the Tresca criterion, aligning better with experimental results for ductile materials, see Fig. 2 [20].

C. Basic Equations of Static Finite Element Analysis

Static finite element analysis (FEM) involves solving for displacements, stresses, and strains in a structure under applied loads. The analysis is governed by the following fundamental equations:

The equilibrium equation relates the external forces acting on the structure to the internal forces arising from stresses:

$$\mathbf{K}\mathbf{u} = \mathbf{f} \tag{5}$$

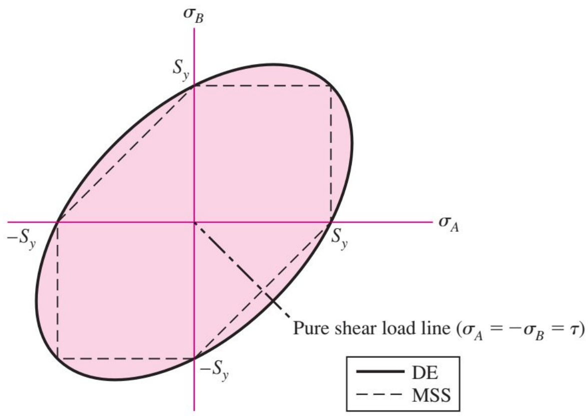

Fig. 2. ®The distortion-energy (DE) theory for plane stress states [20]

where:
- $\mathbf{K}$: Global stiffness matrix, assembled from the element stiffness matrices,
- $\mathbf{u}$: Displacement vector at nodal points,
- $\mathbf{f}$: External force vector.

Strain in an element is related to the displacement vector through the strain-displacement matrix $\mathbf{B}$:

$$\boldsymbol{\varepsilon} = \mathbf{B}\mathbf{u}_e \tag{6}$$

where:
- $\boldsymbol{\varepsilon}$: Strain vector,
- $\mathbf{B}$: Strain-displacement matrix for the element,
- $\mathbf{u}_e$: Nodal displacement vector for the element.

Stress is computed from the strain using the material's constitutive relation:

$$\boldsymbol{\sigma} = \mathbf{D}\boldsymbol{\varepsilon} \tag{7}$$

where:
- $\boldsymbol{\sigma}$: Stress vector,
- $\mathbf{D}$: Material property matrix (elastic modulus and Poisson's ratio),
- $\boldsymbol{\varepsilon}$: Strain vector.

The primary outputs of static FEM analysis are the stress and strain matrices, computed at each element or integration point: Strain Matrix:

$$\boldsymbol{\varepsilon} = \begin{bmatrix} \varepsilon_x & \varepsilon_y & \varepsilon_z & \gamma_{xy} & \gamma_{yz} & \gamma_{zx} \end{bmatrix}^T \tag{8}$$

- $\varepsilon_x, \varepsilon_y, \varepsilon_z$: Normal strains,
- $\gamma_{xy}, \gamma_{yz}, \gamma_{zx}$: Shear strains.

Stress Matrix:

$$\boldsymbol{\sigma} = \begin{bmatrix} \sigma_x & \sigma_y & \sigma_z & \tau_{xy} & \tau_{yz} & \tau_{zx} \end{bmatrix}^T \tag{9}$$

- $\sigma_x, \sigma_y, \sigma_z$: Normal stresses,
- $\tau_{xy}, \tau_{yz}, \tau_{zx}$: Shear stresses.

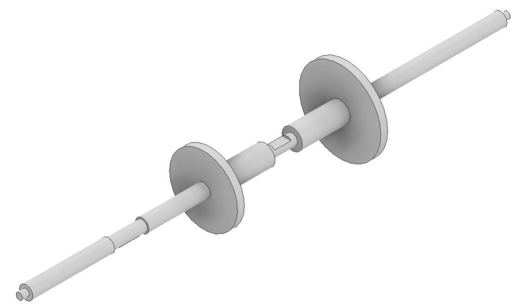

Fig. 3. Solid model of the initial shaft design: Not drawn to scale.

D. Undamped Finite Element Vibration Analysis

In structural vibration analysis, the behavior of a system can be described in terms of its natural frequencies and mode shapes. For undamped systems, the FEM provides a powerful numerical framework to calculate these dynamic properties. The equation of motion for an undamped system in matrix form is expressed as:

$$\mathbf{M}\ddot{\mathbf{u}} + \mathbf{K}\mathbf{u} = \mathbf{0} \tag{10}$$

where:
- $\mathbf{M}$ is the mass matrix,
- $\mathbf{K}$ is the stiffness matrix,
- $\mathbf{u}$ is the displacement vector,
- $\ddot{\mathbf{u}}$ is the acceleration vector.

Assuming harmonic motion, $\mathbf{u}(t) = \boldsymbol{\phi} e^{i\omega t}$, and substituting into the equation yields:

$$\left(\mathbf{K} - \omega^2\mathbf{M}\right)\boldsymbol{\phi} = \mathbf{0} \tag{11}$$

where:
- ω is the natural frequency,
- $\boldsymbol{\phi}$ is the mode shape.

The above equation is an eigenvalue problem:

$$\det\left(\mathbf{K} - \omega^2\mathbf{M}\right) = 0 \tag{12}$$

Solving this equation provides:
- Natural frequencies (ω),
- Mode shapes ($\boldsymbol{\phi}$).

The natural frequencies are the characteristic frequencies at which the structure resonates, while the mode shapes describe the deformation pattern of the structure at each frequency. The FEM approach involves meshing the structure, assembling the global $\mathbf{M}$ and $\mathbf{K}$ matrices, and solving the eigenvalue problem numerically to determine ω and $\boldsymbol{\phi}$.

E. Cost Function Formulation

The cost function J is designed to minimize deviations from desired performance metrics, including von Mises failure criterion, deformation, natural frequencies, mode shapes, and support reactions. The formulation is as follows:

$$J = w_1 J_{\text{von Mises}} + w_2 J_{\text{def}} + w_3 J_{\text{freq}} + w_4 J_{\text{mode}} + w_5 J_{\text{reac}} \tag{13}$$

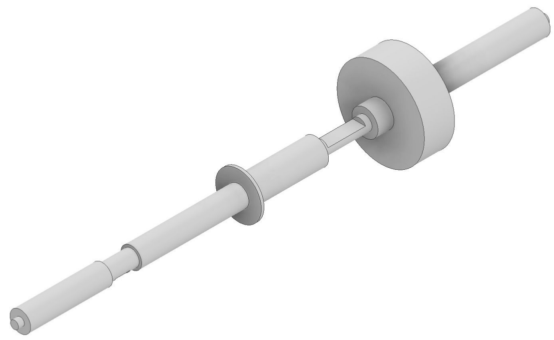

Fig. 4. Solid model of the optimized shaft design: Not drawn to scale.

where:
- $J_{\text{von Mises}}$: Penalization for violating von Mises failure Criterion,
- J_{def}: Penalization for exceeding maximum deformation,
- J_{freq}: Penalization for deviation from desired natural frequencies,
- J_{mode}: Penalization for deviation of mode shapes from desired shapes,
- J_{reac}: Penalization for deviation of support reactions from desired values,
- w_1, w_2, w_3, w_4, w_5: Weights for each term to prioritize specific objectives.

The von Mises criterion is satisfied when the maximum von Mises stress remains below the yield strength σ_y. The penalization term is given by:

$$J_{\text{von Mises}} \quad = \quad (\max \sigma_{von\, Mises})^2 \tag{14}$$

$$\text{if } \max(\sigma_{von\, Mises}) > \sigma_y, \text{ else } 0 \tag{15}$$

To ensure the maximum deformation δ_{max} is below a critical value δ_c:

$$J_{\text{def}} = (\delta_{\text{max}} - \delta_c)^2 \quad \text{if } \delta_{\text{max}} > \delta_c, \text{ else } 0 \tag{16}$$

The natural frequencies ω_i are matched to desired values $\omega_{i,\text{desired}}$ with quadratic penalization:

$$J_{\text{freq}} = \sum_{i=1}^{n} \left(\frac{\omega_i - \omega_{i,\text{desired}}}{\omega_{i,\text{desired}}} \right)^2 \tag{17}$$

The mode shapes $\boldsymbol{\phi}_i$ are compared to desired mode shapes $\boldsymbol{\phi}_{i,\text{desired}}$. The deviation is penalized using a norm-based approach:

$$J_{\text{mode}} = \sum_{i=1}^{n} \left[1 - \frac{\boldsymbol{\phi}_i^T \boldsymbol{\phi}_{i,\text{desired}}}{\|\boldsymbol{\phi}_i\| \|\boldsymbol{\phi}_{i,\text{desired}}\|} \right] \tag{18}$$

Support reactions R_i are constrained to predefined values $R_{i,\text{desired}}$:

$$J_{\text{reac}} = \sum_{i=1}^{m} \left(\frac{R_i - R_{i,\text{desired}}}{R_{i,\text{desired}}} \right)^2 \tag{19}$$

This cost function ensures that all criteria are met by penalizing deviations from desired values. The weights $w_1, \ldots, w_5$ allow prioritization of different objectives based on the design requirements.

V. Numerical Results: Shaft Design

The optimization of the shaft design was performed using an integrated framework that integrates parametric CAD modeling, FEA and multi-objective optimization. Both ends of shaft are fixed. $10MPa$ pressure is applied on the flat surfaces and $50MPa$ traction forces act on cylinder surfaces in opposite directions. Target natural frequencies are set as 1.2 times of original first six natural frequencies. Maximum Von Mises stress and displacement is minimized. The particular cost function for shaft design is:

$$J = w_1 J_{\text{von Mises}} + w_2 J_{\text{def}} + w_3 J_{\text{freq}} \tag{20}$$

Weights of the cost function are: $w_1 = 10^4; w_2 = 1; w_3 = 10^6$. Population size is 50. The GA optimization parameters and material properties are:

options = optimoptions('ga', 'PopulationSize', populationSize, 'InitialPopulationMatrix', initialPopulation, 'Display', 'iter', 'UseParallel', false, 'PlotFcn','gaplotbestf','gaplotbestindiv','OutputFcn', @trackGAProgress, 'MaxGenerations',25, 'MaxStallGenerations', 5);

structuralProperties(modelFEM, 'YoungsModulus', 200×10^3 *,'PoissonsRatio', 0.3, 'MassDensity', 8000* $\times 10^{-9}$*)*

The initial and optimized shaft designs are illustrated in Figures 3 and 4, respectively. The optimization aimed to minimize stress concentrations, reduce deformation, and improve natural frequency separation while ensuring assembly compatibility and structural integrity. The initial and optimized shaft dimensions are presented in Figure 5, highlighting key geometric adjustments made during the optimization process. These modifications include:

- Reduced shaft weight: By optimizing the diameter distribution along the length, material was removed from low-stress regions while reinforcing high-stress areas.
- Improved transition zones: Fillet radii and key geometric transitions were redesigned to reduce stress concentrations.
- Balanced mass distribution: Ensuring better dynamic performance by minimizing mass imbalance and inertia variations.

These improvements resulted in a more efficient material distribution, enhancing the shaft's mechanical and dynamic behavior without compromising structural integrity.

The FEA results for the initial and optimized designs reveal significant improvements in mechanical performance. The von Mises stress criterion, as detailed in the Theory section (Equation 3), was used to evaluate stress levels (Figures 6 and 7).

The displacement analysis (Figures 8 and 9) shows that the optimized shaft design exhibits significantly reduced deformation compared to the initial configuration. The optimization ensured that: $\delta_{\max} \leq \delta_{\text{critical}}$ where $\delta_{\max}$ is the maximum displacement, and δ_{critical} is the allowable limit. The reduction in deformation ensures better assembly compatibility, preventing misalignment that could lead to bearing failures or excessive vibration.

This improvement is particularly beneficial in high-speed rotating applications, where excessive deflection can result in vibration-induced failures and mechanical misalignment. The dynamic response of the shaft was analyzed by solving the eigenvalue problem. The comparison of initial and optimized natural frequencies (Figure 10) demonstrates that the optimized design achieves a more desirable modal response, reducing deviations from target values. This is crucial in rotating machinery, where resonance phenomena must be avoided to ensure stable operation.

The optimized shaft exhibits higher mode separation, meaning that the first few natural frequencies are well spaced, reducing the risk of resonant amplification due to operational harmonics.

The Genetic Algorithm (GA) was employed for optimization, and its performance is summarized in Figures 11-13. The results indicate:

- A steady reduction in the objective function value over iterations (Figure 10), demonstrating progressive improvement in shaft performance.

- A decline in the mean fitness value, signifying enhanced solution quality (Figure 11).

- A reduction in fitness standard deviation, suggesting solution convergence and population stability (Figure 12).

These results validate the efficacy of the proposed optimization approach, ensuring that the final shaft design meets structural and functional constraints while enhancing mechanical efficiency.

The final optimized shaft design achieves: Lower stress concentrations ; Reduced deformation; Improved natural frequency separation; Optimized material distribution for weight reduction. These enhancements ensure a structurally and dynamically superior design, making the shaft more reliable under operational loads. The integration of computational design techniques, FEA, and meta-heuristic optimization results in a design that is both lightweight and mechanically robust, guaranteeing long-term performance and efficiency.

VI. Conclusion

This study introduced a comprehensive and practically implementable framework for the structural optimization of mechanical components, with a focus on shaft design. The proposed methodology integrates parametric CAD modeling, FEA, and multi-objective meta-heuristic optimization into a unified, iterative workflow. Three key contributions distinguish this work: (1) the simultaneous consideration of structural performance and assembly constraints within a single optimization cost function; (2) the automated coupling of CAD and FEA tools for geometry-update-based simulation

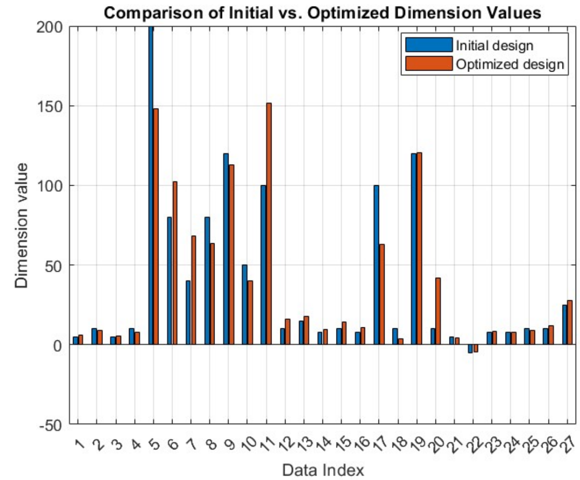

Fig. 5. Comparison of initial and optimized design dimensions (mm).

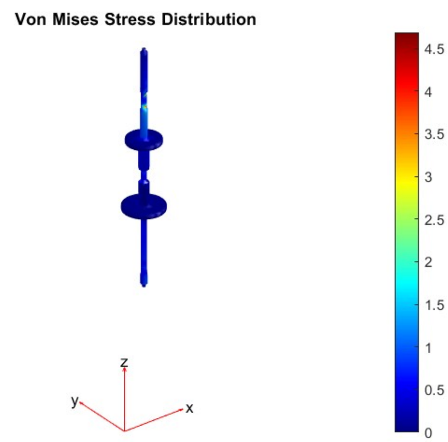

Fig. 6. Initial design von Mises stress (MPa).

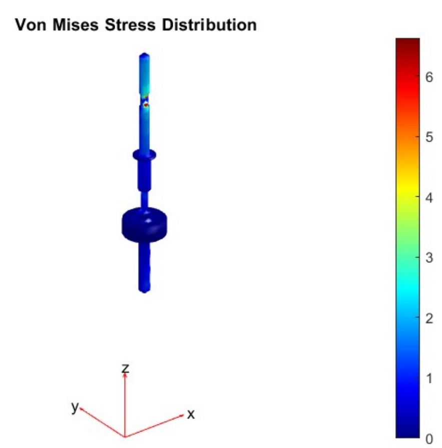

Fig. 7. Optimized design von Mises stress (MPa).

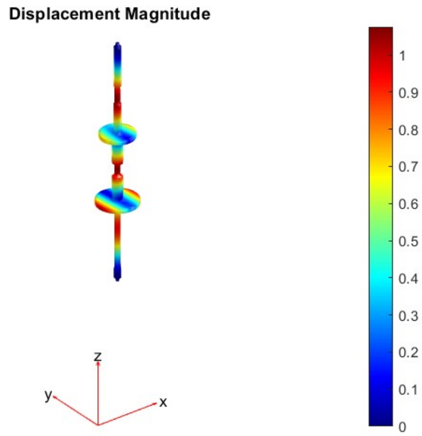

Fig. 8. Initial design displacements (mm).

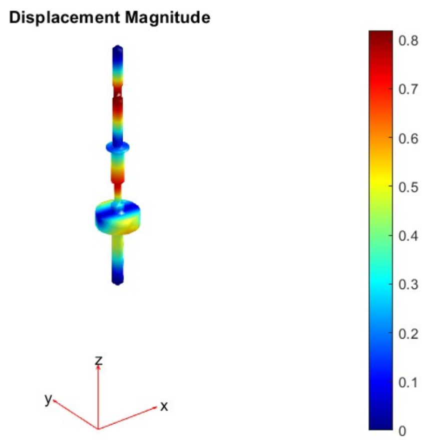

Fig. 9. Optimized design displacements (mm).

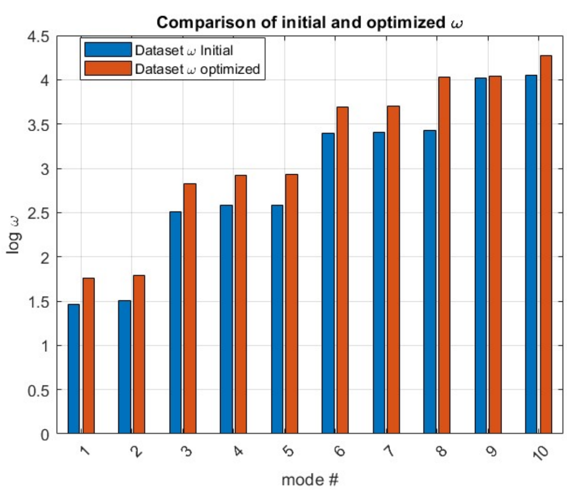

Fig. 10. Comparison of inital and optimized design natural frequencies (Hz).

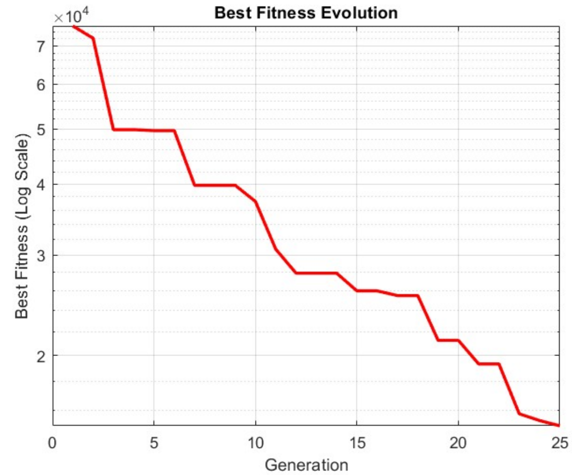

Fig. 11. GA best fitness graph.

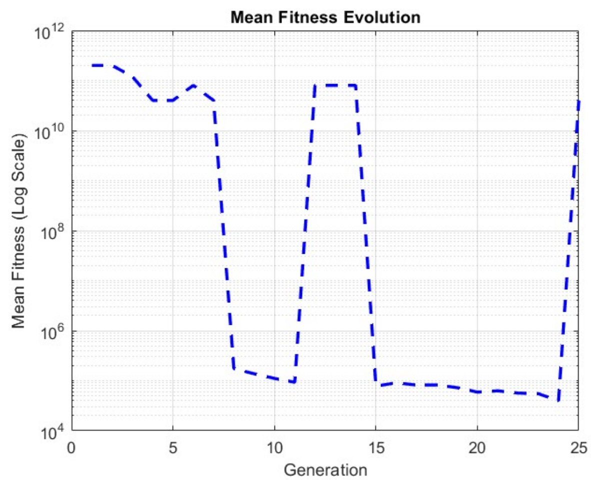

Fig. 12. GA mean fitness graph.

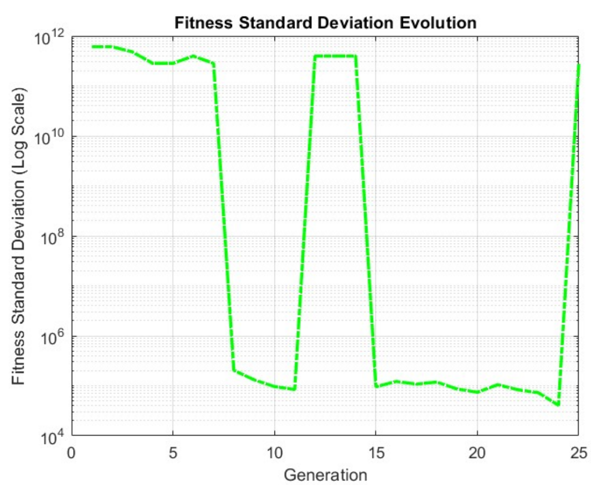

Fig. 13. GA fitness standard deviation graph.

cycles; and (3) the application of this integrated framework to a real-world shaft design problem.

Quantitative results demonstrate the framework's effectiveness: the optimized shaft exhibited a reduction in peak von Mises stress, a decrease in maximum deformation, and an increase in natural frequency separation compared to the baseline design. These improvements ensure greater structural integrity, enhanced vibration resistance, and better assembly compatibility; all crucial for high-speed rotating machinery.

While the case study focused on a shaft component, the framework is readily extendable to other geometrically complex and assembly-sensitive parts such as couplings, brackets, or motor housings. Future work will aim to incorporate manufacturing constraints (e.g., minimum wall thickness, casting limitations), explore the use of surrogate models for faster convergence, and conduct experimental validation on multi-part mechanical assemblies.

REFERENCES

[1] M. P. Bendsøe, "Optimal shape design as a material distribution problem," *Structural optimization*, vol. 1, pp. 193–202, 1989.

[2] O. Sigmund, "Topology optimization: a tool for the tailoring of structures and materials," *Philosophical Transactions of the Royal Society of London. Series A: Mathematical, Physical and Engineering Sciences*, vol. 358, no. 1765, pp. 211–227, 2000.

[3] M. Zhou, N. Pagaldipti, H. Thomas, and Y. Shyy, "An integrated approach to topology, sizing, and shape optimization," *Structural and Multidisciplinary Optimization*, vol. 26, pp. 308–317, 2004.

[4] A. N. Christiansen, J. A. Bærentzen, M. Nobel-Jørgensen, N. Aage, and O. Sigmund, "Combined shape and topology optimization of 3d structures," *Computers & Graphics*, vol. 46, pp. 25–35, 2015.

[5] M. N. K. Kulkarni, M. S. Patekar, M. T. Bhoskar, M. O. Kulkarni, G. Kakandikar, and V. Nandedkar, "Particle swarm optimization applications to mechanical engineering-a review," *Materials Today: Proceedings*, vol. 2, no. 4-5, pp. 2631–2639, 2015.

[6] S. Gupta, H. Abderazek, B. S. Yıldız, A. R. Yildiz, S. Mirjalili, and S. M. Sait, "Comparison of metaheuristic optimization algorithms for solving constrained mechanical design optimization problems," *Expert Systems with Applications*, vol. 183, p. 115351, 2021.

[7] K. Saitou, K. Izui, S. Nishiwaki, and P. Papalambros, "A survey of structural optimization in mechanical product development," 2005.

[8] J. S. Arora, *Optimization of structural and mechanical systems*. World Scientific, 2007.

[9] J. Lu and Y. Chen, "Manufacturable mechanical part design with constrained topology optimization," *Proceedings of the Institution of Mechanical Engineers, Part B: Journal of Engineering Manufacture*, vol. 226, no. 10, pp. 1727–1735, 2012.

[10] L. Pinelli, A. Amedei, E. Meli, F. Vanti, B. Romani, G. Benvenuti, M. Fabbrini, N. Morganti, A. Rindi, and A. Arnone, "Innovative design, structural optimization, and additive manufacturing of new-generation turbine blades," *Journal of Turbomachinery*, vol. 144, no. 1, p. 011006, 2022.

[11] B. Noordman, Y. Ton, J. van den Toorn, M. de Smit, R. Haagsma, T. Koenis, and W. van den Brink, "Topology optimization for the design of a 3d-printed rotating shaft balance," *Progress in Additive Manufacturing*, vol. 8, no. 1, pp. 19–25, 2023.

[12] G. Shanmugasundar, M. Dharanidharan, D. Vishwa, and A. S. Kumar, "Design, analysis and topology optimization of connecting rod," *Materials Today: Proceedings*, vol. 46, pp. 3430–3438, 2021.

[13] C. Li, I. Y. Kim, and J. Jeswiet, "Conceptual and detailed design of an automotive engine cradle by using topology, shape, and size optimization," vol. 51, pp. 547–564.

[14] R. V. Rao, V. J. Savsani, and D. P. Vakharia, "Teaching–learning-based optimization: a novel method for constrained mechanical design optimization problems," *Computer-aided design*, vol. 43, no. 3, pp. 303–315, 2011.

[15] D. Sun, Y. Shi, and B. Zhang, "Robust optimization of constrained mechanical system with joint clearance and random parameters using multi-objective particle swarm optimization," *Structural and Multidisciplinary Optimization*, vol. 58, pp. 2073–2084, 2018.

[16] R. Shinde and S. Sawant, "Optimization of automotive drive shaft for better fuel economy and high torsional strength," *IUP Journal of Mechanical Engineering*, vol. 13, no. 4, pp. 23–35, 2020.

[17] B.-W. Cheng and S. Maghsoodloo, "Optimization of mechanical assembly tolerances by incorporating taguchi's quality loss function," *Journal of Manufacturing Systems*, vol. 14, no. 4, pp. 264–276, 1995.

[18] P.-S. Tang and K.-H. Chang, "Integration of topology and shape optimization for design of structural components," *Structural and Multidisciplinary Optimization*, vol. 22, pp. 65–82, 2001.

[19] L. Li, J. Jiao, S. Sun, Z. Zhao, and J. Kang, "Aerodynamic shape optimization of a single turbine stage based on parameterized free-form deformation with mapping design parameters," vol. 169, pp. 444–455.

[20] R. G. Budynas, J. K. Nisbett, *et al.*, *Shigley's mechanical engineering design*. McGraw-Hill New York, 2011, vol. 9.